Butwal Campus Journal, Vol. 8, No. 2: 1-12, December 2025
Research Management Cell, Butwal Multiple Campus, Tribhuvan University, Nepal
DOI: https://doi.org/10.3126/bcj.v8i2.88209

Investigating the Surface Morphology and Composition of the Methyl Orange by Different Spectroscopic Techniques

Chandradip Kumar Yadav[1,3,4], Susmita Jha[4], Randhir Kumar Jha[2], Benadict Rakesh[3], Adyasha Swain Mohapatra[3], Deepak Nath[4], Madhab Gautam[4,5], Ajaya Bhattarai[6*]

[1]Amrit Campus, Tribhuvan University, Kathmandu, Nepal
[2]Trichandra Multiple Campus, Kathmandu, Nepal
[3]CSIR – Institute of Minerals and Materials Technology, Bhubaneswar-751013, India
[4]Central Department of Chemistry, Tribhuvan University, Kirtipur, Nepal
[5]Department of Chemistry, Tribhuvan Multiple Campus, Tribhuvan University, Palpa, Nepal
[6*] Department of Chemistry, Mahendra Morang Adharsh Multiple Campus, Tribhuvan University, Biratnagar, Nepal
Email: *bkajaya@yahoo.com; ajaya.bhattarai@mmamc.tu.edu.np

Abstract

Weak organic acids and bases function as pH or common anionic indicators for determining the endpoint in neutralization titrations. Methyl orange, a commonly used indicator, appears red in acidic conditions and yellow in alkaline solutions. In this study, surface and spectroscopic analyses were employed to characterize methyl orange. Energy Dispersive X-ray (EDX) analysis was conducted to determine its elemental composition, revealing that approximately 66% of the sample consists of carbon, along with about 24% of oxygen, sulfur, sodium, and other elements. The crystalline nature of the sample was confirmed through X-ray Diffraction (XRD) and Field Emission Scanning Electron Microscope (FE-SEM) analysis. Furthermore, Fourier Transform Infrared (FT-IR) Spectroscopy identified the presence of amino groups and double-bonded carbon atoms within the aromatic system. Raman spectroscopy, particularly in the 1000–1700 cm^{-1} range, further validated the findings from FT-IR. This study serves as a significant contribution to the comprehensive characterization of methyl orange.

Keywords: *anionic indicator, endpoint, methyl orange, neutralization titration.*

Introduction

An organic sulphosalt color called methyl orange has been utilized extensively as an indicator in many different sectors (Nandhini *et al.*, 2019). The possible mechanism of eco-friendly synthesized nanoparticles on hazardous dyes degradation, Biocatalysis, and Agricultural Biotechnology. Methyl Orange is a pH-based indicator that is used because of its clear variance in color when there is a change in pH. It shows a change from orange to red in the acidic medium and yellow in the basic medium. Like other

indicators, it does not have a complete spectrum of color change for various pH levels but has sharp endpoints.

The chemical formula for methyl orange is $C_{14}H_{14}N_3NaO_3S$; its molar mass is 327.33 g/mol, its appearance is yellow or orange solid, and its density is 1.28 g/cm^3 (**Figure 1**). The IUPAC name is sodium-4-[[4-(dimethylamino) phenyl] diazenyl] benzenesulfonate. The excessive usage of this dye leads to several environmental and health hazards (Garg & Chopra, 2021). Reductants like $NaBH_4$ (Sodium borohydride) are being used to reduce methyl orange to small organic molecules and non-toxic compounds. Since the rate of reduction is very slow, metal nanoparticles can accelerate the reaction. Ag-nanoparticles have been extensively used as catalysts in the dye degradation process (Joseph & Mathew, 2014). Fe-nanoparticles synthesized by Trigonella foenum-graecum seeds (Paul et al., 2020) and Ag nanoparticles synthesized using Ulva lactuca (Kumar et al., 2013) were used as catalysts in degrading methyl orange. It is observed that the particle size of Fe in Ag nanoparticles is directly proportional to the reaction time.

The azo group (-N=N-) in methyl orange acts as a chromophore, which is responsible for the strong orange color. In the presence of biologically synthesized ZnO nanoparticles using *Nephelium lappaceum* peel extract, the colour change from strong orange to colorless was observed. This is because of the breaking up of the chromophoric group in the presence of light (Karnan & Selvakumar, 2016). An experiment by Sha *et al.* 2015 showed that hollow Cobalt (Co) nanoparticles easily degraded the dye due to its simple structure and low molecular weight. Co-atoms present on the surface of Co-nanoparticles are likely to access the molecule with low molecular weight and relatively smaller in size. The molecules with higher molecular weight would block the active sites of the catalysts (Sha *et al.,* 2015).

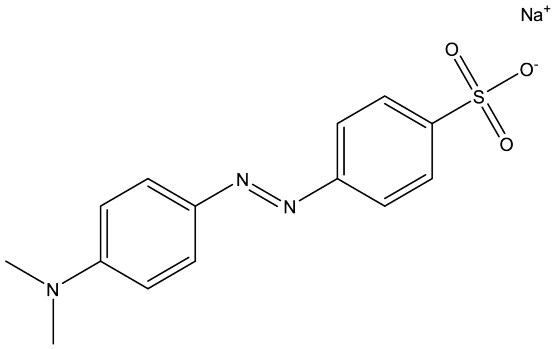

Figure 1: Molecular Structure of Methyl Orange dye

Methyl orange serves as an essential anionic pH indicator, changing color according to acidity and alkalinity, making it valuable for titrations and environmental assessments. It helps determine water quality and pollution levels and is frequently used in photo-catalysis and adsorption studies to examine the removal of organic pollutants (Putri *et al*., 2019). In analytical chemistry, it facilitates spectrophotometric measurements of acids, bases, and metal ions. The dye also contributes to biomedical research by studying drug interactions and cellular uptake. Its role in the textile industry includes

dyeing applications and wastewater treatment. Methyl orange remains significant due to its affordability, accuracy, and ability to support research in wastewater treatment, nanotechnology, and education by demonstrating chemical interactions and equilibrium (Khan *et al.*, 2020).

Methyl orange, as a pH indicator employing surface analytical techniques, has not been extensively researched as far as the author is acquainted. Therefore, detailed surface analysis along with spectroscopic study is a novelty of this work to know dye-related properties of methyl orange. The present study, therefore, aims to investigate surface traits and characteristics by spectroscopic and surface analysis. This work will open the door for future in-depth research on methyl orange.

Materials and method

Materials

Methyl orange (C.I. 13025), CAS No:547-58-0, was purchased from E. Merck (India) Limited.

Methodology

The functional groups present in the fresh crystals of the methyl orange sample were analyzed with ATR mode FT-IR (Bruker alpha II) spectroscopic analysis. The surface morphology of the methyl orange indicator was analyzed using surface imaging techniques with FESEM (JSM-IT800, JEOL), manufactured in Japan, and elemental analysis was carried out with EDAX Octane (Model: Elect Super Energy Dispersive X-ray Spectroscopy, USA) for the compositional analysis. The surface analysis for freshly available methyl orange crystals was performed in different resolutions from 1-10 μm and magnifications. Also, surface analysis of the same crystals was carried out with XRD (Analytical, S.N.: DY 1749) manufactured in the Netherlands. Further, the fresh methyl orange sample was characterized for Raman spectroscopy using a Renishaw spectrometer with λ =532 nm.

Results and Discussion

A Field Emission Scanning Electron Microscope (FE-SEM) is a high-resolution imaging tool that magnifies specimens up to 300,000 times using a focused electron beam. It is particularly effective for analyzing surface morphology and structural characteristics of solid materials. The interaction between the electron beam and the specimen generates secondary electrons, which are displayed on a monitor based on their emission intensity. The quality of the SEM image depends on the elemental composition of the sample, with the higher atomic number of elements producing stronger signals. To enhance imaging, specimens are often coated with high atomic number metals. Additionally, Energy Dispersive X-ray Spectroscopy (EDX) is used to analyze material composition.

In this study, FE-SEM revealed that methyl orange powder consists of irregularly shaped, agglomerated particles with a porous texture. Micrographs, as shown in **Figure 2,** from a FESEM magnify a methyl orange particle. The particle seems to have a rough, layered surface and an uneven, plate-like structure. The surface has noticeable ridges and edges that point to a crystalline or semi-crystalline composition. Numerous tiny protrusions and sometimes even tiny, needle-like crystals or fractures can be seen on the

particle's surface. These characteristics suggest that during the preparation or drying process, the particle may have crystallized or aggregated so that it has some adsorption properties, as described elsewhere (Lázaro Martinez *et al*., 2008).

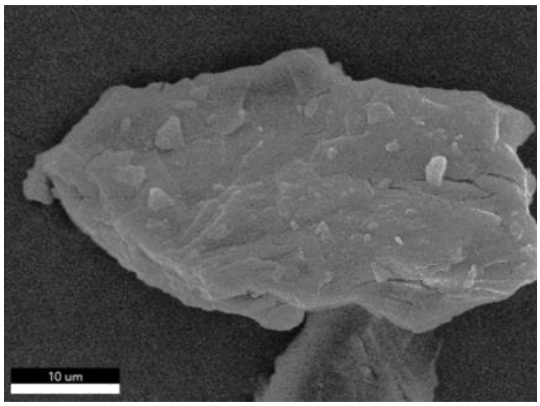

Figure 2: FE-SEM micrographs for the fresh crystals of Methyl orange.

The bottom left scale bar shows that the particle's dimensions are tentatively determined using the given 10 µm scale, placing it in the micrometer range. This demonstrates that the particle size is appropriate for FE-SEM analysis, which is frequently employed for in-depth imaging at this scale. The surface area of a material, which may affect how it behaves in chemical reactions or interactions, may be influenced by its rough texture and irregular shape. The shape of this sample may have an impact on how methyl orange disperses, adsorbs, or reacts with other substances or solvents if it is being used in a study. This FE-SEM image offers important insights into the microscopic morphology and surface properties of methyl orange, which may be pertinent in material synthesis, catalytic processes, or adsorption investigations (Wu *et al.*, 2021). Similarly, surfaces of methyl orange are analyzed using FE-SEM in different resolutions and magnifications, as illustrated in the **Figure. 3**. These micrographs from 1 µm to 10 µm indicate the homogeneity and uniformity of particles present in samples.

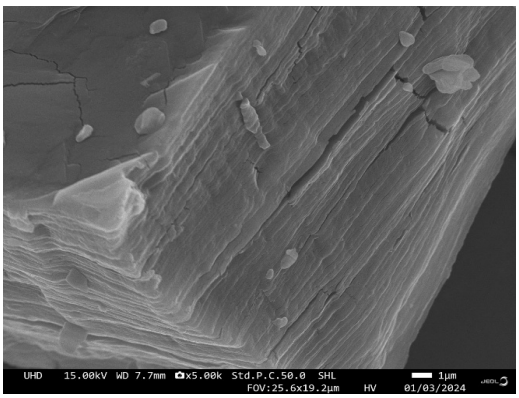

(a)

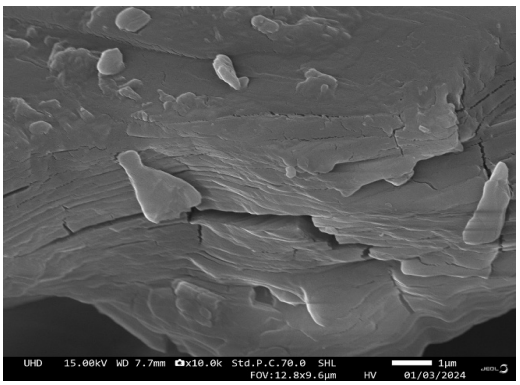

(b)

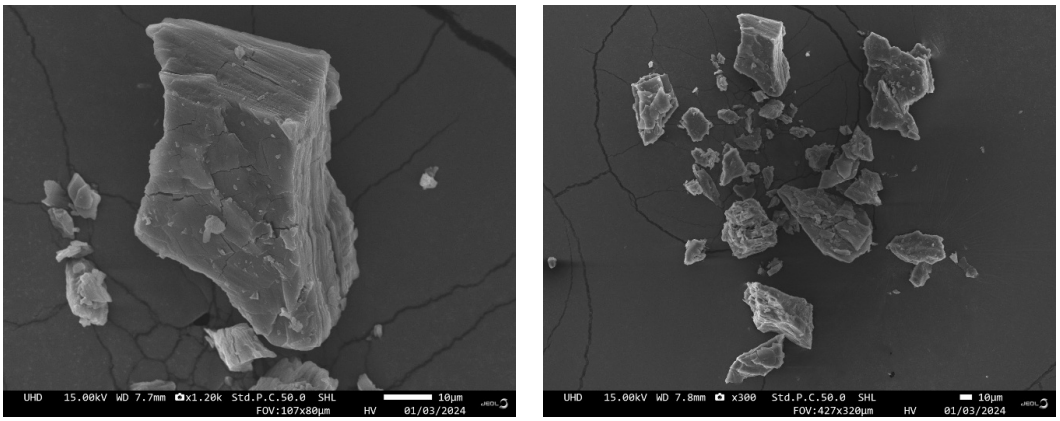

(c) **(d)**

Figure 3: FE-SEM micrographs for methyl orange in different resolutions (1-10 µm) and magnifications (300-10 K).

Energy Dispersive X-ray Spectroscopy (EDX) was utilized, as shown in the **Figure. 4**, to analyze the elemental composition of the methyl orange sample through its characteristic peaks (Newbury & Ritchie, 2013). The findings reveal that carbon (66.3%), oxygen (14.2%), and nitrogen (13.1%) are the primary constituents. The EDX spectrum prominently features a strong carbon peak, confirming it as the most abundant element in the sample. The substantial carbon content (66.3% by weight and 72.9% by atomic percentage) is consistent with previous research. Although oxygen and nitrogen peaks are less intense, they are still distinctly visible, indicating their moderate presence in the sample, as detailed in **Table 1**. Additionally, weaker signals for sodium (Na) and sulfur (S) are detected, corresponding to their lower weight percentages (sulfur: 3.8%, sodium: 2.6%). The predominance of carbon, constituting 66.3% of the sample's weight and 72.9% of its atomic percentage, suggests that the material is carbon-rich. The notable presence of nitrogen and oxygen, each contributing around 13.1% and 14.2% by weight, respectively, further supports this composition. In contrast, sodium and sulfur appear in smaller quantities, with sulfur slightly exceeding sodium in weight percentage while maintaining similar atomic ratios. These differences between weight and atomic percentages are attributed to variations in atomic mass, as lighter elements like carbon exhibit higher atomic percentages compared to heavier elements such as sulfur. Overall, the elemental composition suggests that the sample is primarily organic, with minor amounts of nitrogen, oxygen, sodium, and sulfur, as previously literature (Jini *et al*., 2022). Further, the color mapping study for elements present in the methyl orange sample under investigation validated the occurrence of carbon, nitrogen, oxygen, sodium, and sulfur in the pure sample, depicted in **Figure 5**.

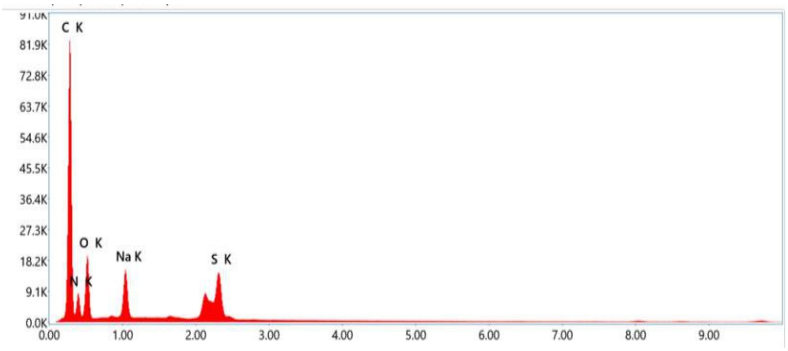

Figure 4: EDX spectra for compositional analysis of fresh crystals of the Methyl orange sample.

Table 1: Elemental composition analysis of Methyl Orange

Element	Weight %	Atomic %
C K	66.3	72.9
N K	13.1	12.3
O K	14.2	11.8
Na K	2.6	1.5
S K	3.8	1.6

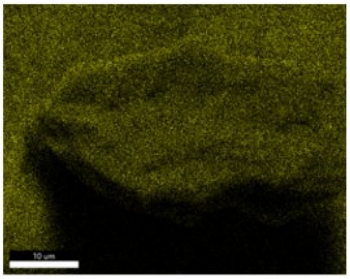

(a)

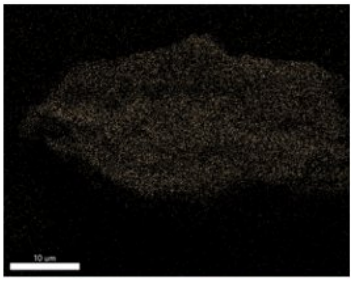

(b)

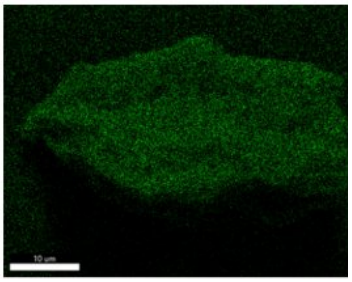

(c)

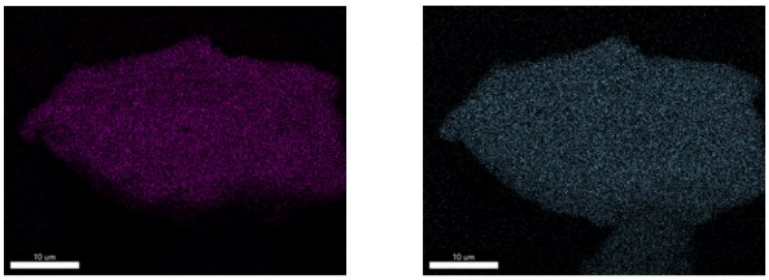

(d) **(e)**

Figure 5: Elemental color mapping analysis of elements (a) Carbon, (b) Nitrogen, (c) Oxygen, (d) Sodium, and (e) Sulphur

X-ray diffraction (XRD) is a widely used non-destructive technique for distinguishing crystalline and amorphous materials, providing insights into lattice parameters and crystallite size through peak positions and intensities (Ali *et al.*, 2022). Strong peaks in the XRD pattern indicated that the samples were crystals. The diffraction peaks were obtained at 2θ values: 20, 25, 27, 30, 32, 36, 41, and 45, corresponding to (111), (012), (121), (130), (032), (212), and (222) planes, respectively, as illustrated in **Figure 6**. The obtained peaks show that Copper gallium sulfide has a tetragonal structure. Pure methyl orange crystals correspond to the orthorhombic crystal system and are therefore confirmed by XRD analysis (Jini *et al*., 2022). This crystalline behaviour of methyl orange is sufficient for adsorption behaviour also (Wu *et al.,* 2021). Due to good adsorption effects, it acts as the best pH indicator.

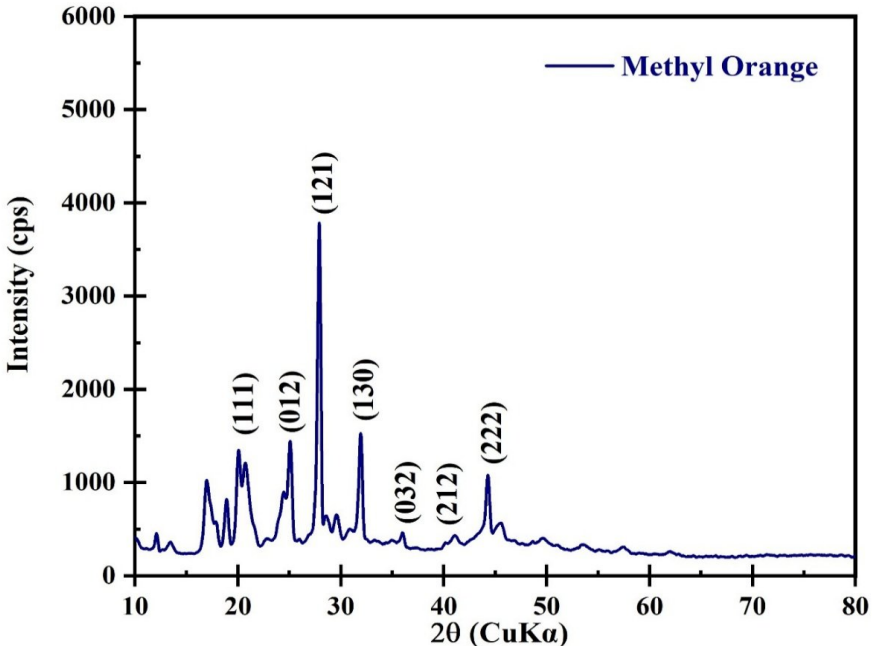

Figure 6: XRD patterns of fresh Methyl orange crystal samples

The functional groups present in the crystalline sample of methyl orange are studied with FT-IR spectroscopic analysis, as displayed in **Figure 7**. The FT-IR spectrum validated the molecular structure of the sample, as shown in **Figure 1,** so that the presence of amine is confirmed by the broad peak near 3400-3500 cm^{-1} (Heacock & Marion, 2011). Also, peaks around 600 cm^{-1} indicated the aromatic systems, and –S=O stretching vibrations indicated by peaks near 1200 cm^{-1}. Peaks at 1600 cm^{-1} and 1516 cm^{-1} for –N=N– stretching vibrations and peaks at 1361 cm^{-1} and 1184 cm^{-1} for –C–N stretching confirm the azo nature of the dye (Kato & Shirai, 2022). Methyl orange displays a peak at 2920 cm^{-1} for asymmetric $–CH_3$ stretching vibrations, peaks at 1676 cm^{-1} and 1646 cm^{-1} represent –C-H bending of aromatic rings (Kalyani *et al.*, 2009).

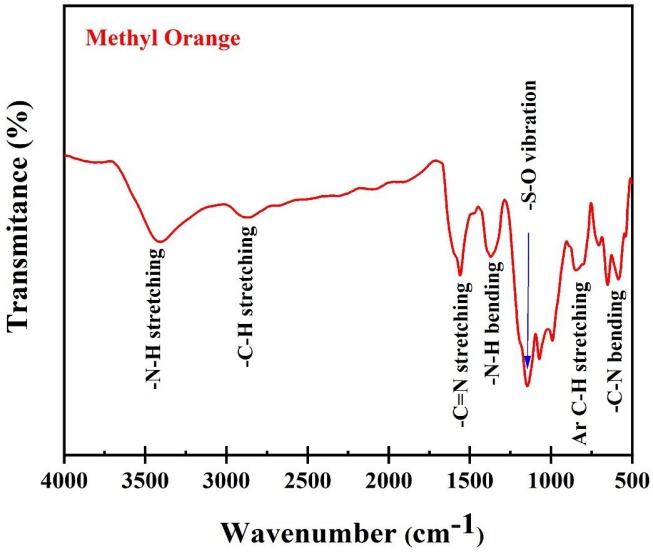

Figure 7: FTIR spectrum for crystals of Methyl orange dye

Raman spectrum analysis provides essential information regarding molecular structure, chemical composition, and molecular interactions (Czaja *et al.*, 2019). The spectra recorded in the 1000–1700 cm^{-1} range, as illustrated in **Figure 8**, reveal characteristic vibrational modes of methyl orange. A distinct peak at 1600 cm^{-1} corresponds to C=C stretching in the aromatic ring. Additionally, strong Raman activity observed near 1400 cm^{-1} is attributed to N=N stretching, characteristic of the azo group. Peaks in the 1000-1200 cm^{-1} range are associated with vibrations of the sulfonate ($–SO_3^-$) group (Adar, 2022).

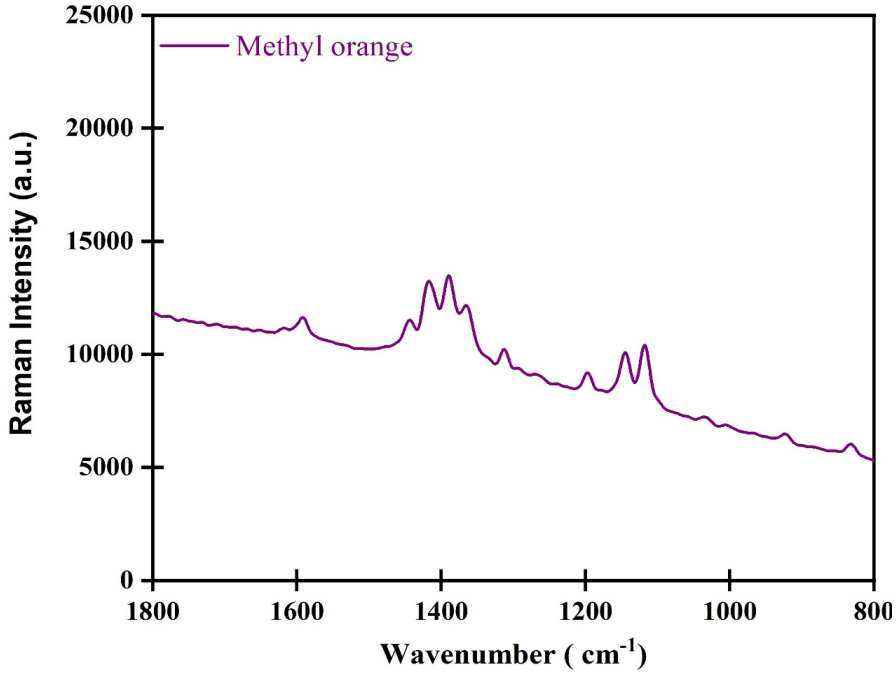

Figure 8: Raman Spectra of Methyl Orange crystals.

The UV-Visible spectroscopic analysis is an important tool to investigate the electronic properties of chemical species. The interactions between dyes (methyl orange, MO) with water are important for altering color, structure, and applications. UV-Visible spectrum of dyes and interaction of dyes with water are analyzed in **Figure 9**. Two peaks are observed with different intensities. One weak peak near 266 nm is due to n→ $\pi*$, and the other strong absorption peaks near 466 nm are due to $\pi\rightarrow \pi*$ (Karunanithi *et al*., 2022).

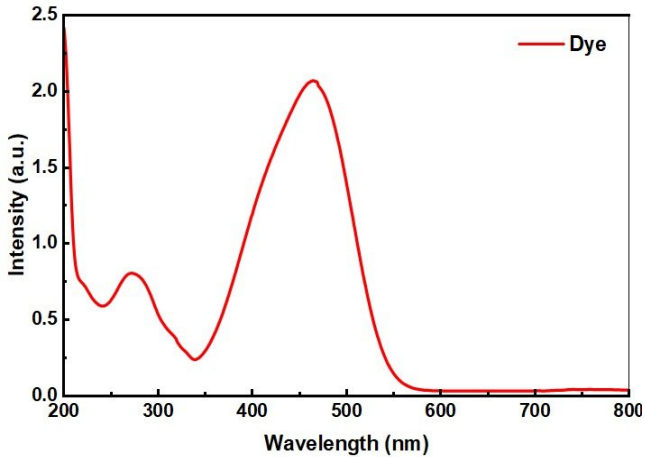

Figure 9: UV-Vis Spectra of Methyl Orange crystals

Though this research revealed the complete elemental, structural, and spectroscopic characterization for fresh crystals of methyl orange dye, it is limited to the analysis of the pure dye under the controlled laboratory environment, as well as in different situations when utilized as catalysts. The present research does not explore how environmental parameters such as pH variability, temperature, or the presence of other competing species may alter its structural stability or structural response. Additionally, the research focuses mainly on characterization, without correlating the findings to adsorption performance, catalytic phenomena, and degradation mechanisms.

Interactions of methyl orange dye in complex aqueous systems or nanomaterials should be investigated in future research. Time-dependent or in-situ analytical techniques should be incorporated to clarify structural changes during degradation or adsorption processes. Also, comparative analysis related to azo dyes, as well as computational modeling of different vibrational modes and bonding, would deepen the understanding of relationships between structure and property. If this researches were performed, the utilization of methyl orange dye for environmental monitoring, wastewater treatment, material-dye interactions, etc., could be investigated.

Conclusion

Organic substances such as weak acids or bases can be used to determine the endpoint in neutralization titrations because they change color under the pH of the solution, making them pH indicators. A frequently used indicator called methyl orange turns yellow in alkaline solutions and red in acidic ones. After determining the elemental composition using Energy Dispersive X-ray (EDX) analysis, it was found that carbon makes up roughly 66% of the sample, with other elements including oxygen, sulfur, and sodium. By using X-ray diffraction (XRD) and Field Emission Scanning Electron Microscope (FE-SEM) analysis, the sample's crystalline nature was verified. Additionally, the aromatic system, double-bonded carbon atoms, and amino groups were detected by Fourier-transform infrared (FT-IR) spectroscopy. Raman spectroscopy Support the FT-IR results, especially in the 1000-1700 cm^{-1} region. This work makes a substantial addition to the thorough characterization of methyl orange.

Acknowledgments

The authors would like to give thanks to INSA for their scholarship and to Scientist Benadict Rakesh of CSIR IMMT for their kind support for this data of FESEM and EDX data from CSIR-IMMT Lab, India.

References

Adar, F. (2022). Interpretation of Raman spectrum of proteins. *Spectroscopy, 37*(2), 9–13, 25. hps://doi.org/10.56530/spectroscopy.lo2270l5

Ali, A., Chiang, Y. W., & Santos, R. M. (2022). X-ray Diffraction Techniques for Mineral Characterization: A Review for Engineers of the Fundamentals, Applications, and Research Directions. *Minerals*, *12*(2), 205. https://doi.org/10.3390/min12020205

Czaja, T., Wójcik, K., Grzeszczuk, M., & Szostak, R. (2019). Polypyrrole–Methyl Orange Raman pH Sensor. *Polymers*, *11*(4), 715. http://dx.doi.org/10.3390/polym11040715

Garg, A., & Chopra, L. (2021). Dye Waste: A significant environmental hazard. *Materials Today: Proceedings*, 48. http://dx.doi.org/10.1016/j.matpr.2021.09.003

Heacock, R. & Marion, L. (2011). The infrared spectra of secondary amines and their salts. *Canadian Journal of Chemistry*, *34*(12), 1782-1795. http://dx.doi.org/10.1139/v56-231

Huang, X., & Zhang, J-Z. (2006). Surfactant-sensitized malachite green method for trace determination of orthophosphate in aqueous solution. *Analytica chimica acta*, 580(1): 55-67. http://dx.doi.org/10.1016/j.aca.2006.07.046

Jini, D., Mani, A., Ajitha, S., Parvathiraja, C., Muniyappan, M., Vivekanand, P., Kamaraj P., Natarajan, A., Almansour, A., Rajangam, A., Raju, S.K., Perumal, K., & Gonfa, G. (2022). Synthesis, Growth, and Characterization of Methyl Orange Dye-Doped Potassium Sulphate Single Crystal and Its Multifaceted Activities. *Advances in Materials Science and Engineering*, *2022*(6), 1-9. http://dx.doi.org/10.1155/2022/4020288

Joseph, S., & Mathew, B. (2014). Microwave-assisted facile synthesis of silver nanoparticles in aqueous medium and investigation of their catalytic and antibacterial activities. Journal of Molecular Liquids, 197, 346–352. http://dx.doi.org/10.1016/j.molliq.2014.06.008

Kalyani, D., Telke, A., Govindwar, S., & Jadhav, J. (2009). Biodegradation and Detoxification of Reactive Textile Dye by Isolated Pseudomonas sp SUK1. *Water Environment Research*, *81*(3), 298-307. http://dx.doi.org/10.2175/106143008X357147

Kato, K., & Shirai, T. (2022). Highly Efficient Water Purification by WO3-based Homo/Heterojunction Photo-catalyst under Visible Light. *Journal of Alloys and Compounds, 901*(2022), 163434. http://dx.doi.org/10.48550/arXiv.2202.06747

Karnan, T., & Selvakumar, S. (2016). Biosynthesis of ZnO nanoparticles using rambutan (*Nephelium lappaceum* L.) peel extract and their photocatalytic activity on methyl orange dye. *Journal of Molecular Structure*, 1125. http://dx.doi.org/10.1016/j.molstruc.2016.07.029

Karunanithi, P., Vigneshwari, R., Paul raj, E., Rajesh, P., Krishnamoorthy, S., & Dash, S. (2022). Pluronic based neutral-ionic binary micellar surfactant systems for solubilizing the cationic methylene blue dye. *Chemical Physics Impact*, 5(1): 100092. http://dx.doi.org/10.1016/j.chphi.2022.100092

Khan, M., Parmar, D.K., & Das, D. (2021). Recent Applications of Azo Dyes: A Paradigm Shift from Medicinal Chemistry to Biomedical Sciences. *Mini-Reviews in Medicinal Chemistry*, *21*(9), 1071-1084. http://dx.doi.org/10.2174/1389557520999201123210025

Kumar, P., Govindaraju, M., Senthamilselvi, S., & Premkumar, K. (2012). Photocatalytic degradation of methyl orange dye using silver (Ag) nanoparticles synthesized from Ulva lactuca. *Colloids and Surfaces B: Biointerfaces*, *103*, 658-661. http://dx.doi.org/10.1016/j.colsurfb.2012.11.022

Lázaro Martínez, J., Denis, M., Piehl, L.L., Celis, E., Buldain, G., & Campo Dall' Orto, V. (2008). Studies on the activation of hydrogen peroxide for color removal in the presence of a new Cu(II)-polyampholyte heterogeneous catalyst. *Applied Catalysis B: Environmental*, *82*(3): 273-283. http://dx.doi.org/10.1016/j.apcatb.2008.01.030

Nandhini, N.T., Shanmugam, R., & Sathiavelu, M. (2019). The possible mechanism of eco-friendly synthesized nanoparticles on hazardous dyes degradation. *Biocatalysis and Agricultural Biotechnology*, *19*(4), 101138. http://dx.doi.org/10.1016/j.bcab.2019.101138

Newbury, D., & Ritchie, N. (2013). Is Scanning Electron Microscopy/Energy Dispersive X-ray Spectrometry (SEM/EDS) quantitative?. *Scanning*, *35*(3). http://dx.doi.org/10.1002/sca.21041

Oudemans, T., Boon, J., & Botto, R. (2007). FTIR and solid-state ^{13}C CP/MAS NMR spectroscopy of charred and non-charred solid organic residues preserved in Roman Iron Age vessels from the Netherlands. *Archaeometry*, *49*(3), 571-294. http://dx.doi.org/10.1111/j.1475-4754.2007.00321.x

Paul, S., Bhowmik, S., Nath, M., Islam, M., Paul, S., Neazi, J., Monir, T., Sabnam, B., Dewanjee, S. & Salam, M. (2020). Silver Nanoparticles Synthesis in a Green Approach: Size Dependent Catalytic Degradation of Cationic and Anionic Dyes. *Oriental Journal of Chemistry*, *36*, 353-360. http://dx.doi.org/10.13005/ojc/360301

Putri, R.A., Safni, S., Jamarun, N., & Septiani, U. (2019). Kinetics Study and Degradation Pathway of Methyl Orange Photodegradation in The Presence of C-N-codoped TiO_2 Catalyst. *Egyptian Journal of Chemistry*, *62* (Part 2), 563-575. http://dx.doi.org/10.21608/ejchem.2019.14543.1883

Sha, Y., Mathew, I., Cui, Q., Clay, M., Gao, F., Zhang, X., & Gu, Z. (2015). Rapid degradation of azo dye methyl orange using hollow cobalt nanoparticles. *Chemosphere*, *144*(2-3), 1530-1535. http://dx.doi.org/10.1016/j.chemosphere.2015.10.040.

Wu, L., Liu, X., Lv, G., Zhu, R., Tian, L., Liu, M., Li, Y., Rao, W., Liu, T., & Liao, L. (2021). Study on the adsorption properties of methyl orange by natural one-dimensional nano-mineral materials with different structures. *Scientific Reports*, *11*(1): 10640. https://www.nature.com/articles/s41598-021-9023.